Electron-phonon interactions in n-type $In_{0.53}Ga_{0.47}As$ and $In_{0.52}Al_{0.48}As$ studied by inelastic light scattering

J. E. Maslar,* J. F. Dorsten, and P. W. Bohn†
Department of Chemistry and Materials Research Laboratory, University of Illinois, 600 South Mathews Avenue, Urbana, Illinois 61801

S. Agarwala and I. Adesida†
Center for Compound Semiconductor Microelectronics, Materials Research Laboratory and Department of Electrical and Computer Engineering, University of Illinois, Urbana, Illinois 61801

C. Caneau and R. Bhat
Bell Communications Research, Red Bank, New Jersey 07701
(Received 1 August 1994)

Room-temperature Raman spectroscopy was used to characterize n-type-doped $In_{0.53}Ga_{0.47}As$ and $In_{0.52}Al_{0.48}As$ layers by observing coupled longitudinal-optical (LO) -phonon-plasmon mode spectra as a function of carrier density. Carrier densities determined from the high-frequency L_+ coupled mode shift in the Raman spectra were compared to carrier densities determined from electrochemical capacitance-voltage profiling measurements. In $In_{0.53}Ga_{0.47}As$ with carrier densities $n \leq 8\times10^{17}$ cm^{-3} accurate determination of carrier densities from the Raman spectra was hindered by Landau damping and small L_+ mode dispersion. Better agreement between the two techniques was observed in $In_{0.53}Ga_{0.47}As$ and $In_{0.52}Al_{0.48}As$ for carrier densities of about 8×10^{17} cm^{-3} and higher, doping levels at which Landau damping is less pronounced. Surface band bending was evaluated from changes in Raman intensity as a function of carrier density of dipole-allowed LO-phonon modes originating in the surface space-charge region. Values for the surface built-in potential determined from the Raman spectra were found to be smaller than those obtained from electrical measurements. The discrepancy is attributed to screening of the surface dipole by photogenerated carriers.

I. INTRODUCTION

$In_xGa_{1-x}As$ and $In_xAl_{1-x}As$ layers are both utilized in the fabrication of high-frequency electronic and long-wavelength photonic devices. The growth of doped layers is a frequent requirement in the production of such devices. It is therefore necessary to characterize the electrical and optical properties of these layers in order to optimize device performance. Unfortunately, it is often difficult to fabricate suitable Schottky contacts for capacitance-voltage (CV) measurements on highly doped III-V semiconductors,[1] making the optical measurement of electrical properties in such materials an attractive alternative. Further, unlike classical electrical measurements, optical techniques can be used as *in situ*, nondestructive, spatially resolved probes of a variety of semiconductor device fabrication steps.[2] Consequently, there is a large impetus for the development of optical probes. Raman spectroscopy is a nondestructive, noncontact technique with the potential for micron spatial resolution, which can be used to study a number of semiconductor material properties. Of particular relevance to this investigation, Raman spectroscopy has been used with success to determine carrier densities and surface band bending in III-V semiconductors, including GaAs, GaP, $Al_xGa_{1-x}As$, and InP.[3-14] However, little has been reported of the electronic properties of doped $In_xGa_{1-x}As$ and $In_xAl_{1-x}As$ layers. Given the importance of the $In_xGa_{1-x}As/In_xAl_{1-x}As$ material system in the fabrication of high-performance electronic and photonic devices, it is very desirable to understand how the light-scattering properties of these materials are related to carrier dynamic properties.

In this investigation, room-temperature Raman spectroscopy was used to characterize n-type-doped $In_{0.53}Ga_{0.47}As$ and $In_{0.52}Al_{0.48}As$ layers. Coupled LO-phonon–plasmon-mode spectra were observed as a function of carrier density. Coupled-mode frequencies were calculated as a function of carrier density using a Drude form of the semiconductor phonon-plasmon dielectric function, including finite wave-vector corrections, but ignoring Landau damping. The carrier densities obtained from the L_+ mode frequency in the Raman spectra were then compared to those obtained from electrochemical CV profiling measurements. In addition, surface band bending was evaluated from changes in intensity as a function of carrier density of the dipole-allowed LO-phonon modes originating in the surface space-charge region (SCR).

II. EXPERIMENT

A. Material preparation

All material was grown lattice matched to an Fe-doped (100) InP substrate. $In_{0.53}Ga_{0.47}As$ (subsequently referred

to as $In_xGa_{1-x}As$) layers were grown by metal-organic chemical-vapor deposition (MOCVD). Nominally undoped material ($n \leq 10^{15}$ cm^{-3}) consisted of a 3000-Å epitaxial $In_xGa_{1-x}As$ layer and n-type-doped material consisted of 1 μm of Si-doped $In_xGa_{1-x}As$. Carrier densities were determined by electrochemical CV profiling to be 2×10^{17}, 8×10^{17}, and 3.5×10^{18} cm^{-3} in the three intentionally doped samples studied. In subsequent discussion carrier densities determined from electrochemical CV profiling are denoted n_{CV} to distinguish them from those determined from the L_+ mode frequency in the Raman spectra, which are denoted n_{RS}. Nominally undoped $In_{0.52}Al_{0.48}As$ (subsequently referred to as $In_xAl_{1-x}As$) layers ($n \leq 10^{15}$ cm^{-3}) were grown by molecular-beam epitaxy and consisted of a 9000-Å layer buffered from the substrate by an $In_xGa_{1-x}As/In_xAl_{1-x}As$ superlattice and another 500-Å layer of $In_xAl_{1-x}As$. Intentionally doped $In_xAl_{1-x}As$ consisted of an MOCVD-grown 1-μm layer of Si-doped $In_xAl_{1-x}As$ with $n_{CV}=2\times10^{18}$ cm^{-3}.

B. Spectroscopic measurements

All Raman spectra were recorded at room temperature in a near-backscattering geometry using a Spex 1877 Triplemate spectrograph with a Photometrics Series 200 charge-coupled device camera system. A Coherent Innova 90-6 Ar^+ laser was used to illuminate samples with either 488- or 514.5-nm radiation. 488-nm excitation is near-resonant with the E_1 critical point in $In_{0.53}Ga_{0.47}As$,[15] but nonresonant for $In_{0.52}Al_{0.48}As$.[16,17] 514.5-nm excitation is nonresonant for both materials. All Raman spectra were recorded with an irradiance of $\sim$270 W/cm^2. A cylindrical lens arrangement was employed to obtain a line focus and thereby minimize the effects in the spectra of sample inhomogeneities and photogenerated carriers. In this investigation the notations x, y, z, x', y', and $\bar{z}$ denote [100], [010], [001], [110], [1$\bar{1}$0], and [00$\bar{1}$], respectively.

III. FREQUENCY DISPERSION CALCULATIONS

A careful evaluation of carrier density measurements by inelastic light-scattering techniques depends critically on accurate frequency dispersion information. In this work we have calculated dispersion with carrier density for both $In_{0.53}Ga_{0.47}As$ and $In_{0.52}Al_{0.48}As$ in the manner described below. If phonon and plasmon damping is weak, then the coupled-mode frequencies ω are given by the zeros of the real part of the dielectric function of the phonon-plasmon system.[12] The dielectric function $\varepsilon(q,\omega)$ for a ternary material can be expressed in the Drude form as[11,18]

$$\varepsilon(q,\omega)=\varepsilon_\infty+\frac{4\pi\rho_1\omega_{TO_1}^2}{\omega_{TO_1}^2-\omega^2-i\gamma_1\omega}+\frac{4\pi\rho_2\omega_{TO_2}^2}{\omega_{TO_2}^2-\omega^2-i\gamma_2\omega}-\varepsilon_\infty\frac{\omega_P^2(q)}{(\omega^2-\frac{3}{5}q^2v_F^2)+i\Gamma\omega}\ , \tag{1}$$

where ε_∞ is the semiconductor high-frequency dielectric constant, $4\pi\rho_i$ is the oscillator strength of the respective binary component, each of which is denoted by i ($i=1,2$); ω_{TO_i} is the TO-phonon frequency, γ_i is the phonon damping constant, Γ is the plasmon damping constant, and v_F is the Fermi velocity given by[12]

$$v_F=\frac{\hbar}{m^*}k_F\ , \tag{2}$$

where $\hbar$ is Planck's constant, m^* is the free-electron concentration-dependent electron effective mass, and k_F is the Fermi wave vector defined as[12]

$$k_F=\sqrt[3]{3\pi^2n}\ , \tag{3}$$

where n is the free-electron density. The q-dependent plasma frequency $\omega_p(q)$ is given by[12]

$$\omega_P^2(q)=\omega_P^2+\tfrac{3}{5}q^2v_F^2\ , \tag{4}$$

where ω_p is the plasma frequency and can be expressed as[18]

$$\omega_P^2=\frac{4\pi ne^2}{\varepsilon_\infty m^*}\ . \tag{5}$$

The wave-vector-dependent term in Eq. (1) is an extension of the Drude form of the dielectric function to account for the spatial dispersion of the plasmon mode, and is developed using the hydrodynamical theory.[19] This approximation is valid when $\omega > qv_F$ and $q < k_F$.[12] The mode oscillator strengths in Eq. (1) can be calculated from the following relationships:[9,18]

$$\omega_{LO_1}^2+\omega_{LO_2}^2=\left[1+\frac{4\pi\rho_1}{\varepsilon_\infty}\right]\omega_{TO_1}^2+\left[1+\frac{4\pi\rho_2}{\varepsilon_\infty}\right]\omega_{TO_2}^2\ , \tag{6}$$

$$\omega_{LO_1}^2\omega_{LO_2}^2=\left[1+\frac{4\pi\rho_1}{\varepsilon_\infty}+\frac{4\pi\rho_2}{\varepsilon_\infty}\right]\omega_{TO_1}^2\omega_{TO_2}^2\ , \tag{7}$$

where ω_{LO_1} and ω_{LO_2} are the LO-phonon frequencies of the respective binary component.

In the determination of the GaAs conduction-band effective mass, the effects of conduction-band nonparabolicity must be considered at free-carrier concentrations of $\sim10^{18}$ cm^{-3} and larger.[20] The same is true of other bulk III-V semiconductors.[21] For this investigation, corrections to the electron effective mass for conduction-band nonparabolicity were made in the manner of Raymond, Robert, and Bernard,[20] using a three-band model, which includes the lowest-lying conduction band and the two highest-lying valence bands. The model is represented by[20]

$$\frac{1}{m^*}=\left[\frac{1}{m_0^*}\right]\left[1-2\frac{\phi}{E_g}\right]\ , \tag{8}$$

where m_0^* is the electron effective mass at the bottom of the conduction band, and ϕ is given by

$$\phi=(3\pi)^{2/3}\frac{(\hbar^2)}{2m_0^*}n^{2/3}\ . \tag{9}$$

IV. RESULTS AND DISCUSSION

A. $In_{0.53}Ga_{0.47}As$

Figure 1 shows the Raman spectra of $In_xGa_{1-x}As$ as a function of doping density excited with 514.5-nm radiation in the $z(x,y)\bar{z}$ geometry. Under the $q=0$ approximation, only deformation-potential and electro-optic (interband Fröhlich) LO-phonon scattering is allowed in the backscattering configuration from the (100) surface of a zinc-blende crystal.[22] This results in the observation of two LO-phonon modes for ternary crystals which exhibit two-mode behavior, such as $In_{0.53}Ga_{0.47}As$ (Refs. 23 and 24) and $In_{0.52}Al_{0.48}As$.[25] Figure 1(a) shows the spectrum of nominally undoped $In_xGa_{1-x}As$. LO-phonon modes corresponding to an InAs-like LO-phonon mode and a GaAs-like LO-phonon mode are observed at 233.6 and 269.5 cm^{-1}, respectively. In addition, a peak is observed at 245 cm^{-1} which is attributed to an alloy disorder mode and denoted R^* after the notation of Estrera *et al.*[26] Also seen are second-order modes denoted by $2O$. Figures 1(b), 1(c), and 1(d) show the spectra of the samples with carrier densities of $n_{CV}=2\times10^{17}$, 8×10^{17}, and 3.5×10^{18} cm^{-3}, respectively. All of these spectra exhibit the phonon modes observed in Fig. 1(a). In addition, peaks attributed to coupled LO-phonon–plasmon-modes are present. In doped polar semiconductors, the LO-phonon modes can couple with the collective plasmon mode. For ternary semiconductors which exhibit two-mode behavior this results in three coupled modes,[7–9,11] denoted L_-, L_0, and L_+, representing the low-, intermediate-, and high-frequency coupled modes, respectively. Scattering by both unscreened LO-phonon modes and coupled phonon-plasmon modes arises due to the presence of a SCR. In the absence of free carriers, scattering originating from the SCR approximates scattering from an undoped bulk crystal. When the penetration depth of the exciting radiation is greater than the width of the SCR, a combination of scattering from the unscreened LO-phonon mode (in the SCR) and the coupled modes (from the underlying region where free carriers are still present) is observed.

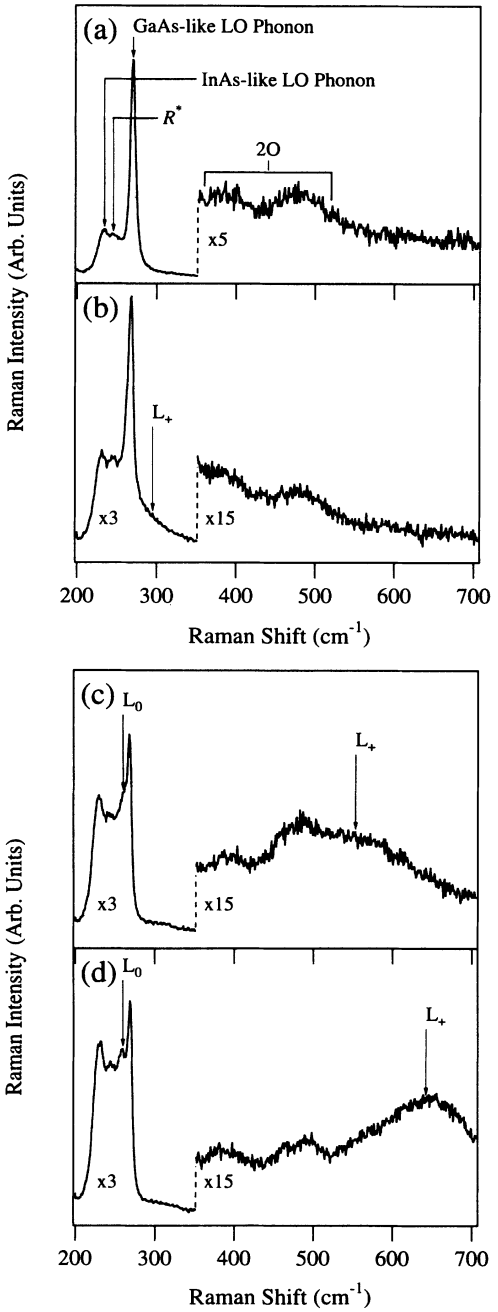

FIG. 1. The Raman spectra of $In_xGa_{1-x}As$ as a function of doping density excited with 514.5-nm radiation in the $z(x,y)\bar{z}$ geometry. (a), (b), (c), and (d) show the spectra of the nominally undoped $n_{CV}=2\times10^{17}$, 8×10^{17}, and 3.5×10^{18} cm^{-3} layers, respectively. All spectra are shown on the same intensity scale.

No scattering attributed to the L_- modes is identified in the spectra of any of the doped samples. Nash, Skolnick, and Bass[23] have reported that the electron-phonon coupling is weaker for the InAs-like LO phonon than the GaAs-like LO phonon, which could contribute to the absence of the L_- peak. An examination of the coupled-mode dispersions suggests additional possible explanations. The calculated and measured coupled-mode frequencies are summarized in Table I and are displayed in Fig. 2 along with the calculated dispersion as a function of carrier density (solid lines) for $In_{0.53}Ga_{0.47}As$. Also shown are the phonon frequencies (dotted lines), $\omega_p(q)$ (dashed line), and the boundary of the single-particle excitation (SPE) continuum, ω_{SPE}, (dashed-dotted line), which will be discussed subsequently. The measured coupled-mode frequencies for doped $In_xGa_{1-x}As$ with 2×10^{17} $cm^{-3}\leq n_{CV}\leq3.5\times10^{18}$ cm^{-3} are also displayed. TO-phonon frequencies of $\omega_{TO_1}=225$ cm^{-1} and $\omega_{TO_2}=255$ cm^{-1}, as determined from the $In_xGa_{1-x}As$ phonon dispersion reported by Estrera *et al.*[26] were used, and values of $\varepsilon_\infty=11.61$,[27] $E_g=0.75$ eV,[15] and $m_0^*/m_e=0.041$,[21] where m_e is the rest mass of an electron, were also employed. A value of 4.45 for the real index of refraction (514.5-nm excitation) (Ref. 28) was used to calculate $q=1.09\times10^6$ cm^{-1}.

It is clear from Fig. 2 and Table I that the experimental and calculated values of the coupled-mode frequencies are not always in strong agreement. There are a number of potential limitations of Raman-scattering measure-

TABLE I. Measured and calculated coupled phonon-plasmon mode frequencies for n-type $In_xGa_{1-x}As$.

n_{CV}	n_{RS}	Measured coupled-mode frequency (cm^{-1})			Calculated coupled-mode frequency (cm^{-1})		
(10^{17} cm^{-3})	(10^{17} cm^{-3})	L_-	L_0	L_+	L_-	L_0	L_+
2.0±1.0	0.35		~270	~290	224	251	382
8.0±4.0	8.50		261.3	554	228	257	569
35.0±17.5	12.00		258.7	644	227	256	773

ments which could contribute to this discrepancy. The determination of n_{RS} is based upon the relationship of the coupled-mode frequencies to the free-carrier density via the plasmon-mode dispersion. Obviously, obtaining an accurate value of n_{RS} depends on accurately modeling the plasmon dispersion and plasmon-phonon interactions. Relatively simple models have been used to generate the coupled-mode dispersions. Some characteristics of these models which could contribute to the discrepancies between the calculated and measured mode frequencies include the neglect of finite temperature in the calculations of the coupled-mode frequencies and the use of only the lowest-lying conduction band in the model describing the carrier density dependence of the electron effective mass. In addition, to simplify the coupled-mode calculations, plasmon and phonon damping, e.g., due to alloy disorder, were neglected. This was justified because good agreement has been reported between experimental and calculated coupled-mode frequencies for $Al_xGa_{1-x}As$.[8,11] Presumably, similar contributions to phonon and plasmon damping, in particular those due to alloy disorder, would occur in $In_xGa_{1-x}As$, $In_xAl_{1-x}As$, and $Al_xGa_{1-x}As$. An effect which cannot be treated with the models employed here is Landau damping of the plasma, i.e., limitation of the lifetime of the collective plasma excitations due to decay into single-particle excitations. Hence, when ω is within the frequency limits of the SPE continuum, the hydrodynamical model can be a poor description of the dielectric function.[12] The boundaries of the SPE continuum are given by[4]

$$\omega_{SPE}=\frac{\hbar}{2m^*}q^2\pm qv_F \ . \tag{10}$$

The dispersion of the SPE continuum in Fig. 2 indicates that Landau damping should be considered for $In_xGa_{1-x}As$, particularly for the L_0 and L_- modes whose frequencies lie within the SPE continuum. For this reason, the difference in n_{CV} and n_{RS} for the epilayer with $n_{CV}=2\times10^{17}$ cm^{-3} is attributed to Landau damping. Landau damping could also contribute to the absence of the L_- modes and the L_0 mode in Fig. 1(b). On the other hand, the absence of the L_- modes also could be due to the small frequency split between the InAs-like TO- and LO-phonon modes, which makes it difficult to resolve a third mode of intermediate frequency. This type of argument could also contribute to the absence of the L_0 mode in Fig. 1(b). The proximity of L_0 to the InAs-like LO phonon, the R^* mode, and the GaAs-like TO phonon makes resolution of the L_0 mode difficult.

Based on the simple model of the SPE continuum presented, it is expected that Landau damping should have a smaller effect on layers with higher carrier densities. Therefore, in the absence of other effects, n_{CV} and n_{RS} should be in better agreement for samples with higher doping levels. Indeed, for values of $n_{CV}=8\times10^{17}$ and 3.5×10^{18} cm^{-3} the CV and Raman-scattering measurements agree reasonably well, given the large uncertainty associated with the CV measurement. The uncertainty associated with these CV measurements was estimated to be 50%; however, a factor of 2 error is possi-

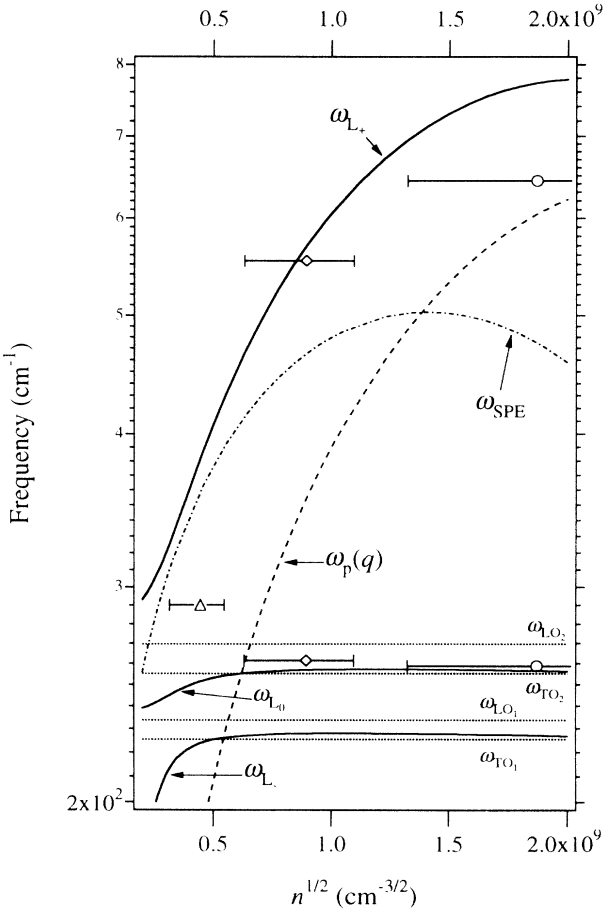

FIG. 2. The calculated coupled-mode frequencies in $In_xGa_{1-x}As$ as a function of carrier density (——). Also shown are the phonon frequencies (· · · ·), $\omega_p(q)$ (— — —), ω_{SPE} (—·—·—·), and the coupled-mode frequencies determined from the Raman spectra for $In_xGa_{1-x}As$ with $n_{CV}=2\times10^{17}$ cm^{-3} (△), 8×10^{17} cm^{-3} (◇), and 3.5×10^{18} cm^{-3} (○).

ble in some cases. In addition to uncertainties associated with the CV measurements, discrepancies between n_{CV} and n_{RS} could arise due to the limited probe depth of the Raman-scattering measurement. For 514.5-nm excitation the optical probe depth in crystalline $In_{0.53}Ga_{0.47}As$ is $\sim 1/\alpha = 445$ Å,[18] with a corresponding Raman escape depth of $1/2\alpha = 223$ Å. The first point probed by these CV measurements ranges from $\sim 200-2000$ Å from the surface for the highest to the lowest doping levels, respectively. Hence, even for the epilayers with the highest doping levels, the region probed by the first point of the CV profiling measurement is as deep or deeper than the whole region probed by the Raman-scattering measurement. Therefore, while the CV measurements are influenced by diffusion of carriers originating in the region of the crystal probed by the Raman-scattering measurements, these two measurements are, in effect, probing different regions of the crystal (for the conductions, i.e., excitation wavelength, of this investigation). It is well established that unintentional hydrogen passivation of dopants can occur in III-V semiconductors as a result of a variety of processing steps including vapor-phase epitaxy,[29] although to our knowledge no such passivation of Si-doped $In_xGa_{1-x}As$ has been reported. This type of effect could lead to a gradient in the carrier density at the surface with the effect being that the Raman-scattering measurements were probing a region of the crystal with a carrier density lower than that of the bulk. Obviously, the presence of this effect could be verified quite simply by exciting Raman scattering with longer-wavelength radiation which has a correspondingly deeper probe depth.

While it is clear that the coupled-mode spectra are determined by a complex interaction of a number of factors, the following conclusions can be drawn. (1) The absence of the L_- mode is attributed to Landau damping and/or weak electron–InAs-like-LO-phonon coupling. (2) The discrepancy between the observed and calculated L_0 mode frequencies for all samples and the L_+ mode frequency for $In_xGa_{1-x}As$ with $n_{CV} = 2\times 10^{17}$ cm^{-3} is due to Landau damping. (3) Landau damping has less effect on the L_+ mode frequencies for $In_xGa_{1-x}As$ with $n_{CV} = 8\times 10^{17}$ and 3.5×10^{18} cm^{-3} and, consequently, the agreement between n_{CV} and n_{RS} is better.

The SCR width W_s can be investigated through a detailed examination of the relative intensities of the unscreened LO-phonon modes. For this investigation the GaAs-like LO-phonon mode was used, since it was the most intense peak in the spectrum. The GaAs-like LO-phonon intensity was normalized to the R^* mode intensity, since R^* is related to alloy disorder and should not be affected by the magnitude of the surface SCR. The Raman intensity of the unscreened LO-phonon scattering originating in the surface SCR, I_{LO}, is given by[3]

$$I_{LO} = I_{LO}^0 (1 - e^{-2\alpha W_S}) , \tag{11}$$

where I_{LO}^0 is the total LO-phonon mode intensity for a crystal with no SCR, and α is the absorption coefficient of the incident radiation. The SCR width of a one-sided abrupt junction (assuming a carrier distribution tail rather than a step distribution) can be expressed as[30]

$$W_S = \left[\frac{2\varepsilon_{s0}\varepsilon_0 (V_{Bi} - k_B T/e)}{en} \right]^{1/2} , \tag{12}$$

where ε_{s0} is the semiconductor static dielectric constant, ε_0 is the permittivity of free space, V_{Bi} the built-in potential, $k_B T/e$ is the thermal voltage, k_B is the Boltzmann constant, and T is the absolute temperature.

Figure 3 shows the measured LO-phonon intensities normalized to the appropriate R^* mode intensity from the spectra of the intentionally doped $In_xGa_{1-x}As$ layers. For the $n_{CV} = 2\times 10^{17}$-cm^{-3} $In_xGa_{1-x}As$ sample, n_{CV} was used in determining both points. Also shown is the calculated LO-phonon intensity as a function of carrier density using the measured value of I_{LO}^0 from the spectrum of nominally undoped $In_xGa_{1-x}As$ and a value of W_s calculated from Eq. (12). Values of $\alpha = 2.249\times 10^5$ cm^{-1} (514.5-nm excitation) (Ref. 28) and $\varepsilon_{s0} = 13.94$ (Ref. 27) were used for these calculations. A value of $V_{Bi} = 0.07$ V produces the dashed curve. Morkoç, Drummond, and Stanchak[31] reported $V_{Bi} = 0.3$ V at 78 K for Au Schottky dots on n-type $In_{0.53}Ga_{0.47}As$ ($n = 10^{17}$ cm^{-3}), which corresponds to $V_{Bi} \sim 0.28$ V at room temperature. The fact that the V_{Bi} value determined from the Raman-scattering measurement is smaller than those reported from CV measurements is attributed to photogenerated carriers. The effects of the incident photon flux, particularly screening of the surface dipole by photogenerated carriers, is an important consideration when evaluating band bending from Raman spectra.[3] Screening of the surface dipole leads to a value of V_{Bi}, determined from Raman measurements, which is somewhat smaller than the value obtained in the dark. Notably, however, the fact that scattering by unscreened phonon modes is observed indicates that a SCR still exists.

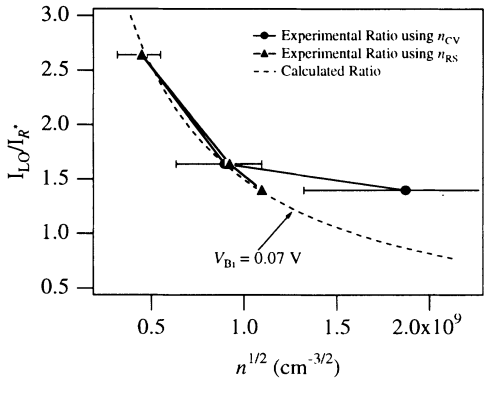

FIG. 3. The measured intensity ratios of LO phonons normalized to the respective R^* mode for the intentionally doped $In_xGa_{1-x}As$ layers as a function of n_{CV} (●) and n_{RS} (▲). Also shown is the calculated LO-phonon intensity as a function of carrier density (— — —) using the measured value of I_{LO}^0 from the spectrum of nominally undoped $In_xGa_{1-x}As$ and a value of W_s calculated from Eq. (12) with $V_{Bi} = 0.07$ V.

B. $In_{0.52}Al_{0.48}As$

Figure 4 shows the Raman spectra of n^--$In_xAl_{1-x}As$ and n^+-$In_xAl_{1-x}As$ ($n_{CV}=2\times10^{18}$ cm^{-3}) excited with 488-nm radiation in the $z(x,y)\bar{z}$ geometry. The inset shows the spectrum on an expanded intensity scale. The InAs-like and AlAs-like LO-phonon modes are observed at $\omega_{LO_1}=233.4$ cm^{-1} and $\omega_{LO_2}=365.6$ cm^{-1}, respectively. The low-frequency asymmetric broadening of the AlAs-like LO-phonon mode has been observed in $Al_xGa_{1-x}As$ spectra and is due to a disorder-induced increase in the range of phonon wave vectors participating in Raman scattering.[32] Despite the similarities, these spectra exhibit important differences attributed to electron-phonon coupling, including (1) a broad peak identified as the L_+ mode, which is observed at ~475 cm^{-1} in the n^+-$In_xAl_{1-x}As$ spectrum; and (2) an asymmetric low-frequency broadening of the InAs-like mode observed in the n^+-$In_xAl_{1-x}As$ spectrum relative to that of the n^--$In_xAl_{1-x}As$ spectrum resulting from L_- mode scattering.

Figure 5 shows the Raman spectra of n^--$In_xAl_{1-x}As$ and n^+-$In_xAl_{1-x}As$ excited with 488-nm radiation in the $z(x,x)\bar{z}$ geometry. In this geometry, impurity-induced LO-phonon scattering can be observed in addition to other forbidden extrinsic mechanisms and intrinsic mechanisms,[33] although scattering due to many of these mechanisms is difficult to observe without resonant excitation. The *DALA* peak ascribed to disorder-activated longitudinal-acoustic-phonon scattering has been previously identified in $In_xAl_{1-x}As$.[25] The peaks labeled "disorder-induced" are attributed to scattering associated with the LO-phonon modes due to alloy-disorder-induced lowering of the crystal symmetry. In particular, the broad asymmetric peak at ~360 cm^{-1} corresponds to the low shift shoulder on the AlAs-like LO phonon in the spectrum recorded in the $z(x,y)\bar{z}$ geometry. Although leakage from the dipole-allowed scattering probably contributes, if leakage from the dipole-allowed scattering were the primary mechanism a bigger difference in scattering intensities would be observed. It is clear that the presence of the dopant does not result in a measurable difference in these spectra. Although it is possible that the dipole-allowed LO-phonon modes are more sensitive to crystal perturbation than the peaks in the $z(x,x)\bar{z}$ geometry, it is reasonable to assign the broadening of the InAs-like LO-phonon mode in the n^+-$In_xAl_{1-x}As$ spectrum to L_- mode scattering, rather than dopant-induced disorder effects. It is not known why L_- mode scattering is observed, and L_0 mode scattering is not in n^+-$In_xAl_{1-x}As$ spectrum, while the opposite is the case for the n-type $In_xGa_{1-x}As$ spectra. However, the large phonon character of the L_0 mode coupled with the relatively low scattering efficiency of the AlAs-like LO-phonon mode probably contributes to its absence.

Figure 6 shows the $In_{0.52}Al_{0.48}As$ coupled-mode frequencies as a function of carrier density (solid lines) determined by setting Eq. (1) equal to zero. Again, an n-dependent electron effective mass corrected for conduction-band nonparabolicity was employed. For these calculations values of $E_g=1.45$ eV (Ref. 17) and $m_0^*/m_e=0.075$ (Ref. 34) were used. $\varepsilon_\infty=10.29$ was determined from the ε_∞ values for InAs and AlAs (Ref. 35) through a linear interpolation method as described in Ref. 36. No peaks attributed to the TO-phonon modes were observed in these spectra, so the ω_{TO} values were approximated in the following manner. In $Al_xGa_{1-x}As$ the LO-phonon frequencies and TO-phonon frequencies of the respective two-mode components converge as the composition is varied from one to the other binary constituent.[37] Assuming that this is also the case with $In_{1-x}Al_xAs$, the $In_xAl_{1-x}As$ LO-phonon dispersion as a function of Al composition was obtained from the work of Emera *et al.*[25] The LO- and TO-phonon frequencies of the respective binary constituents were obtained from Ref. 35. The dispersion of the TO-phonon frequencies as a function of composition was then determined, and the LO-TO-phonon splitting for $In_xAl_{1-x}As$ was obtained. This frequency splitting was then used to estimate the TO-phonon frequency in the material utilized in this work from the measured LO-phonon frequencies. Values of $\omega_{TO_1}=222$ cm^{-1} and $\omega_{TO_2}=345.6$ cm^{-1} were deter-

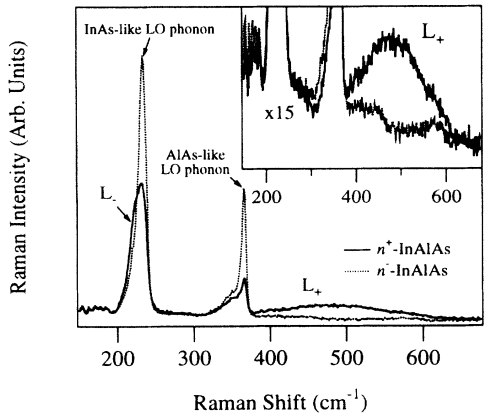

FIG. 4. The Raman spectra of n^--$In_xAl_{1-x}As$ and n^+-$In_xAl_{1-x}As$ in the $z(x,y)\bar{z}$ geometry. The inset shows the spectrum on an expanded intensity scale.

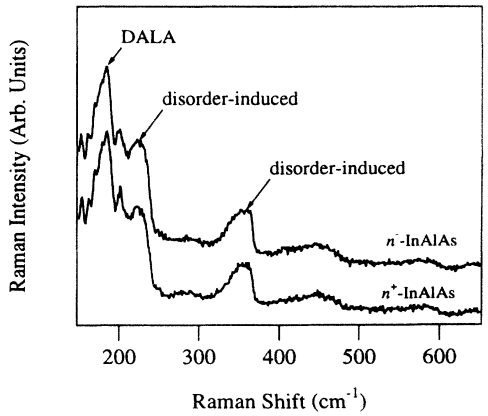

FIG. 5. The Raman spectra of n^--$In_xAl_{1-x}As$ and n^+-$In_xAl_{1-x}As$ in the $z(x,x)\bar{z}$ geometry.

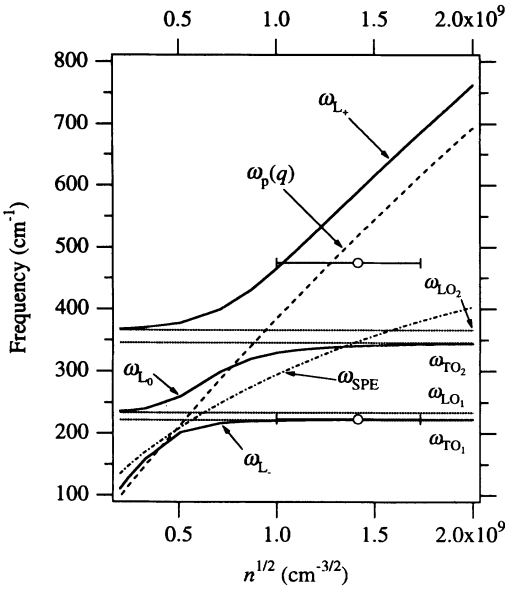

FIG. 6. The calculated coupled-mode frequencies of $In_xAl_{1-x}As$ as a function of carrier density (——). Also shown are the phonon frequencies (· · · ·), $\omega_p(q)$ (— — —), ω_{SPE} (—·—·—·), and the coupled-mode frequencies determined from the Raman spectrum of n^+-$In_xAl_{1-x}As$ and using $n_{CV}=2\times10^{18}$ cm^{-3} (○).

mined by this method. A value of 4.08 for the real index of refraction (488-nm excitation) (Ref. 38) was used to calculate $q=1.05\times10^6$ cm^{-1}.

Figure 6 shows that for $n_{CV}=2\times10^{18}$ cm^{-3} the L_- and L_0 mode frequencies are located very near the respective TO-phonon frequencies. This is consistent with the assignment of the low-frequency scattering associated with the InAs-like LO phonon to the L_- mode. As was the case in $In_xGa_{1-x}As$, the measured L_+ mode frequency is in reasonable agreement with the mode frequency calculated using $n_{CV}=2\times10^{18}$ cm^{-3}, given the large uncertainty of the CV measurement. The measured L_+ mode frequency corresponds to $n_{RS}=1.1\times10^{18}$ cm^{-3}.

Again, the magnitude of W_S and, therefore, V_{Bi}, can be estimated from the relative intensities of the unscreened LO-phonon modes in the spectra of n^--$In_xAl_{1-x}As$ and n^+-$In_xAl_{1-x}As$ (cf. Fig. 4). Since the InAs-like LO-phonon mode was the most intense in the spectra, it was used for the determination of W_S. The InAs-like LO-phonon mode was normalized to the $DALA$ mode intensity, since the $DALA$ mode is disorder related and not dependent on the magnitude of the SCR. From the spectra in Fig. 4, a value of $W_S=200$ Å, which corresponds to a value of $V_{Bi}=0.35$ V (using n_{RS}) was determined for the n^+-$In_xAl_{1-x}As$ layer. A value of $\alpha=2.16\times10^5$ cm^{-1} (488-nm excitation) (Ref. 35) was used for this calculation. $\varepsilon_{s0}=12.42$ was determined from the ε_{s0} values for InAs and AlAs (Ref. 35) through a linear interpolation method as described in Ref. 36. Sadwick *et al.*[39] have reported values of $V_{Bi}=0.49$–0.65 V for various Schottky contacts on $In_{0.52}Al_{0.48}As$ ($n=2.35$–2.6×10^{16} cm^{-3}), which is in reasonable agreement with the V_{Bi} values determined from the Raman spectra. Again, the fact that the V_{Bi} value determined from the Raman measurement is somewhat smaller than those reported from CV measurements is attributed to the effects of photogenerated carriers.

V. CONCLUSIONS

The coupled phonon-plasmon modes in n-type-doped $In_{0.53}Ga_{0.47}As$ and $In_{0.52}Al_{0.48}As$ layers were examined as a function of carrier density using Raman spectroscopy. Carrier densities determined from the L_+ mode frequency in the Raman spectra were compared to the carrier densities determined from electrochemical CV profiling measurements. It was demonstrated that carrier densities could be obtained from the Raman spectra with an accuracy comparable to electrochemical CV profiling for crystals with doping levels of $n\geq8\times10^{17}$ cm^{-3}, where the effects of Landau damping are relatively small. For crystals with $n\leq8\times10^{17}$ cm^{-3}, accurate determination of carrier densities from the Raman spectra was hindered by Landau damping and small L_+ mode dispersion. Potentially, one could improve the accuracy of the Raman-scattering determination of doping density for crystals with lower doping levels by exciting scattering with longer-wavelength radiation. First, longer-wavelength radiation has a smaller value of q and, therefore, at a given coupled-mode frequency the effects of Landau damping would be less significant. Second, the greater penetration depth associated with longer-wavelength radiation would result in more scattering originating from beneath the SCR. From the changes in unscreened dipole-allowed LO-phonon intensities as a function of carrier density, the built-in potentials of $In_{0.53}Ga_{0.47}As$ were determined to be 0.07 and 0.35 V, respectively. These numbers are smaller than values obtained from C^{-2} vs V data due to the effects of photogenerated carriers on the Raman spectra.

ACKNOWLEDGMENTS

J.E.M. wishes to thank J. J. Kopanski of the NIST Semiconductor Electronics Division for helpful discussions concerning CV measurements. This work was supported by the National Science Foundation through Grant No. ECD 89-43166 and by the Office of Naval Research through Grant No. N00014-93-1-1168.

*Present address: Chemical Science and Technology Laboratory, National Institute of Standards and Technology, Gaithersburg, MD 20899.

†Authors to whom correspondence can be addressed.

[1]D. W. Palmer, in *Growth and Characterization of Semiconductors*, edited by R. A. Stradling and P. C. Klipstein (Institute of Physics, New York, 1990), p. 194.

[2]D. E. Aspnes, R. Bhat, C. Caneau, E. Colas, L. T. Florez, S. Gregory, J. P. Harbison, I. Kamiya, V. G. Keramidas, M. A. Koza, M. A. A. Pudenski, W. E. Quinn, S. A. Schwarz, M. C.

Tamargo, and H. Tanaka, J. Cryst. Growth **120**, 71 (1992).
[3]J. Geurts, Surf. Sci. Rep. **18**, 1 (1993).
[4]B. Boudart, B. Prévot, and C. Schwab, Appl. Surf. Sci. **50**, 295 (1991).
[5]S. Nakashima, H. Yugami, A. Fujii, M. Hangyo, and H. Yamanaka, J. Appl. Phys. **64**, 3067 (1988).
[6]B. H. Bairamov, I. P. Ipatova, V. A. Milorava, V. V. Toporov, K. Naukkarinen, T. Tuomi, G. Irmer, and J. Monecke, Phys. Rev. B **38**, 5722 (1988).
[7]T. Yuasa and M. Ishii, Phys. Rev. B **35**, 3962 (1987).
[8]D. Kirillov, Y. Chai, C. Webb, and G. Davis, J. Appl. Phys. **59**, 231 (1986).
[9]T. Yuasa, S. Naritsuka, M. Mannoh, K. Shinozaki, K. Yamanaka, Y. Nomura, M. Mihara, and M. Ishii, Phys. Rev. B **33**, 1222 (1986).
[10]H. Shen, F. H. Pollak, and R. N. Sacks, Appl. Phys. Lett. **47**, 891 (1985).
[11]R. J. Becker, P. F. Luehrmann, and D. W. Langer, Appl. Phys. Lett. **47**, 513 (1985).
[12]A. Abstreiter, M. Cardona, and A. Pinczuk, in *Light Scattering in Solids,* edited by M. Cardona and G. Güntherodt (Springer-Verlag, Heidelburg, 1984), Vol. IV, p. 5.
[13]G. Abstreiter, E. Bauser, A. Fischer, and K. Ploog, Appl. Phys. **16**, 345 (1978).
[14]D. T. Hon and W. L. Faust, Appl. Phys. **1**, 241 (1973).
[15]S. Adachi, *Physical Properties of III-V Semiconductor Compounds* (Wiley, New York, 1992), p. 75.
[16]J. M. Rodríguez and G. Armelles, J. Appl. Phys. **69**, 965 (1991).
[17]B. Wakefield, M. A. G. Halliwell, T. Kerr, D. A. Andrews, G. J. Davies, and D. R. Wood, Appl. Phys. Lett. **44**, 341 (1984).
[18]O. K. Kim and W. G. Spitzer, Phys. Rev. B **20**, 3258 (1979).
[19]U. Nowak, W. Richter, and G. Sachs, Phys. Status Solidi B **108**, 131 (1981).
[20]A. Raymond, J. L. Robert, and C. Bernard, J. Phys. C **12**, 2289 (1979).
[21]S. Adachi, *Physical Properties of III-V Semiconductor Compounds* (Ref. 15), p. 86.
[22]M. Cardona, in *Light Scattering in Solids,* edited by M. Cardona and G. Güntherodt (Springer-Verlag, New York, 1982), Vol. II, p. 19.
[23]K. J. Nash, M. S. Skolnick, and S. J. Bass, Semicond. Sci. Technol. **2**, 329 (1987).
[24]K. P. Jain, R. K. Soni, S. C. Abbi, and M. Balkanski, Phys. Rev. B **32**, 1005 (1985).
[25]S. Emura, T. Nakagawa, S. Gonda, and S. Shimizu, J. Appl. Phys. **62**, 4632 (1987).
[26]J. P. Estrera, P. D. Stevens, R. Glosser, W. M. Duncan, Y. C. Kao, H. Y. Liu, and E. A. Beam III, Appl. Phys. Lett. **61**, 1927 (1992).
[27]S. Adachi, *Physical Properties of III-V Semiconductor Compounds* (Ref. 15), p. 63.
[28]S. Adachi, *Properties of Indium Phosphide* (INSPEC, London, 1991), p. 416.
[29]S. J. Pearton, C. R. Abernathy, W. S. Hobson, F. Ren, T. R. Fullowan, J. Lopata, U. K. Chakrabarti, M. Stavola, and D. M. Kozuch, Mater. Sci. Eng. **13**, 171 (1992).
[30]S. M. Sze, *Physics of Semiconductor Devices,* 2nd. ed. (Wiley, New York, 1981), p. 74.
[31]H. Morkoç, T. J. Drummond, and C. M. Stanchak, IEEE Trans. Electron Dev. **ED-28**, 1 (1981).
[32]B. Jusserand and J. Sapirel, Phys. Rev. B **24**, 7194 (1981).
[33]W. Kauschke and M. Cardona, Phys. Rev. B **33**, 5473 (1986).
[34]D. Olego, T. Y. Chang, E. Silberg, E. A. Caridi, and A. Pinczuk, Appl. Phys. Lett. **41**, 476 (1982).
[35]O. Madelung, W. von der Osten, and U. Rössler, in *Semiconductors. Intrinsic Properties of Group IV Elements and III-V, II-VI, and I-VII Compounds,* edited by O. Madelung, Landolt-Bornstein, New Series, Group 3, Vol. 22, Pt. a (Springer-Verlag, Berlin, 1982).
[36]S. Adachi, J. Appl. Phys. **53**, 8775 (1982).
[37]F. H. Pollak, in *Properties of Aluminum Gallium Arsenide,* edited by S. Adachi (INSPEC, London, 1993) p. 30.
[38]H. W. Dinges, H. Burkhard, R. Lösch, H. Nickel, and W. Schlapp, Appl. Surf. Sci. **54**, 477 (1992).
[39]L. P. Sadwick, C. W. Kim, K. L. Tan, and D. C. Streit, in *Gallium Arsenide and Related Compounds 1991,* edited by G. B. Stringfellow, IOP Conf. Ser. No. 120 (Institute of Physics and Physical Society, London, 1992), Chap. 4, p. 211.